Journal of the European Ceramic Society 22 (2002) 2269–2275

www.elsevier.com/locate/jeurceramsoc

Microstructural and mechanical behaviour of polyamide fibre-reinforced plaster composites

S. Eve[a], M. Gomina[a,*], A. Gmouh[b], A. Samdi[b], R. Moussa[b], G. Orange[c]

[a]*Equipe Structure et Comportement Thermomécanique des Matériaux, ESCTM/CRISMAT, UMR 6508 du CNRS, ISMRA 6 Bd du Maréchal Juin 14050 Caen Cedex, France*

[b]*Equipe Microstructure et Physico-Chimie des Matériaux, UFR Physico-Chimie des Matériaux (C 53/97), Université Hassan II, Faculté des Sciences Aïn Chock B.P.5366 Maârif, Casablanca, Morocco*

[c]*Groupe Renforcement-Matériaux, Rhodia Recherches, 93308 Aubervilliers Cedex, France*

Received 20 August 2001; received in revised form 12 December 2001; accepted 28 December 2001

Abstract

Different concentrations of polyamide fibres with given aspect ratios were associated to a commercial plaster in a view to investigate the mechanical behaviour. The presence of these water-absorbent fibres perturbs the hydration of the plaster and causes changes in the plaster microstructure. All the mechanical parameters decrease monotonically as the concentration of fibres is increased, except the fracture toughness which shows a different trend. The ability of the composites to retain strength at the onset of matrix cracking has been forecast and analysed on a phenomenological basis in terms of a fibre efficiency factor which is a useful supplement to the usual mechanical characterisation of such materials.

Keywords: Acoustic emission; Composites; Fibres; gypsum; Plaster; Mechanical properties

1. Introduction

Due to its availability in subsoil, a relative low cost, a high use easiness and mechanical characteristics suitable for many employments, plaster is a widely used construction material. However plaster appears heavy, permeable (which forbids exterior applications) and too brittle. Heaviness and brittleness may be appreciably reduced by combining plaster with mineral particles[1] or natural fibres.[2–4] Particularly, number of studies have shown that glass fibre-reinforced plaster materials possess appreciable toughness values,[5–7] but the high cost of these fibres is a handicap for their association with a such cheap material like plaster at an industrial scale. In this paper, we have investigated the mechanical behaviour of a commercial plaster reinforced with polyamide fibres, with emphasize to the influences of the concentration and the aspect ratio of the fibres.

2. Materials

The starting powder is a commercially available gypsum (Plaster of Paris, hemihydrated calcium sulphate, termed LAMBERT LUTECE 80) designed for interior applications. To check the influences of the aspect ratio of the reinforcement, different batches of polyamide fibres (PA) supplied by Rhodia (Centre d'Aubervilliers, France) with diameters 15 and 40 μm and lengths 1.2, 6 and 12 mm were used. The nominal values of the Young's modulus and the tensile strength are 2 GPa and 500 MPa, respectively, and the ultimate tensile strain is 200%.

Samples of set plaster were prepared using a consistency of 0.68, which is close to the typical water/dry materials ratio used in building applications.

On the basis of a previous study on hair reinforced-plaster,[2] we have chosen fibre concentrations of 0.1, 0.2, 0.5, 1, 2 and 5 wt.%. The fibres were scattered in water before the gypsum was added, and these constituents were mixed according to a given protocol.

Specimens of standard dimensions 160×40×40 mm and specimens of dimensions 160×20×10 mm were prepared using a rigid polyvinylchloride mould. The

* Corresponding author.
E-mail address: moussa.gomina@ismra.fr (M. Gomina).

0955-2219/02/$ - see front matter
PII: S0955-2219(02)00014-6

temperature rise, during the plaster setting, relatively to the actual room temperature, was monitored by means of an ultra thin platinum probe inserted into the mould through a lateral face. The volume change of the materials during the setting was qualitatively appreciated by measuring the upward pressure exerted on a plate in contact with the top face of the specimen. All the samples were air-cured for 24 h at room temperature before drying in an oven at 40 °C for 7 days.

The different types of composites were referenced xPRy/z where:

x is the fibre diameter (15 or 40 μm)
PR stands for "reinforced-plaster"
y represents 10 times the fibre length ($y=12$, 60 or 120)
z is 10 times the concentration of fibres ($z=1$, 2, 5, 10, 20 and 50).

As an example, a sample referenced 40PR60/20 contains 2 wt.% of fibres 6 mm long and 40 μm of diameter.

3. Experimental procedure

The smooth specimens of dimensions 160×40×40 mm were loaded in three point bending (span over width $L/W \approx 4$) at a crosshead displacement rate of 3 mm/min, by means of a Schenck type testing machine equipped with a 10 kN load cell. The stress–strain curves of these specimens were used for the evaluation of the flexural strength, σ_R, and the associated first damage strain, ε_R [Eq. 1); while the loading curves of the specimens of dimensions 160×20×10 mm were used for the estimation of the Young's modulus, E [Eq. 2]. The compression strength, σ_c, was measured on specimens of dimensions $l=80$ mm, $B=40$ mm and $W=40$ mm loaded by means of two steel plates [Eq. (3)]. Specimens with a single edge notch a_0 were loaded to rupture for the fracture toughness measurement from the experimental fracture stress σ_t, with a loading configuration L/W≈4 and a notch over depth ratio $a_0/W=0.35$ [Eq. (4)].

$$\varepsilon_R = \frac{6Wh}{L^2};\quad \sigma_R = \frac{3}{2}\frac{LF_R}{BW^2} \tag{1}$$

$$E = \frac{\Delta F}{\Delta h}\left(\frac{L}{W}\right)^3 \frac{1}{4B} \tag{2}$$

$$\sigma_c = \frac{F}{S} \tag{3}$$

$$K_{IC} = \sigma_t Y\sqrt{a_0} \tag{4}$$

A Mistras acoustic emission set, with a total amplification of 80 dB, and equipped with a 25–625 kHz bypass piezoelectric transducer, was used to correlate the total acoustic emission counts to the loading curves for damage threshold and damage mechanisms analysis. The surfaces of rupture were gold-sputtered for microscopy observations by means of a Philips FEG scanning electron microscope.

4. Results and discussion

4.1. Characterisation of the neat plaster

Hydration of plaster gives a crystalline porous product consisting of a tangle of randomly orientated needle-like small crystallites (about 5 μm) and larger particles (Fig. 1). This closely interlocked crystalline framework and the remaining porosity determine the mechanical properties of the set plaster.

A typical 3 point bending stress-strain curve depicted in Fig. 2 emphasizes the linear elastic behaviour up to catastrophic failure at the point ($\varepsilon_R=0.43\%$, $\sigma_R=3.1$

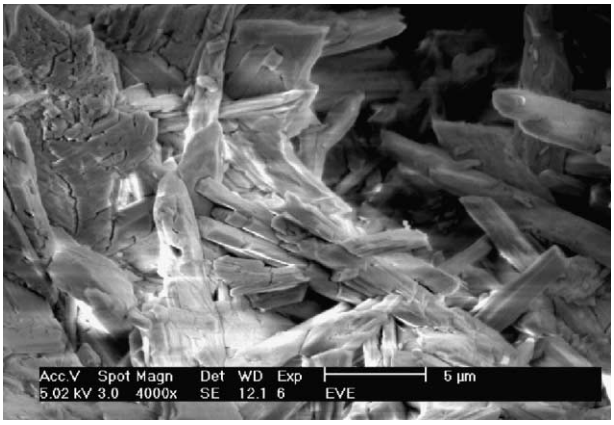

Fig. 1. Needle-like structure of the neat plaster.

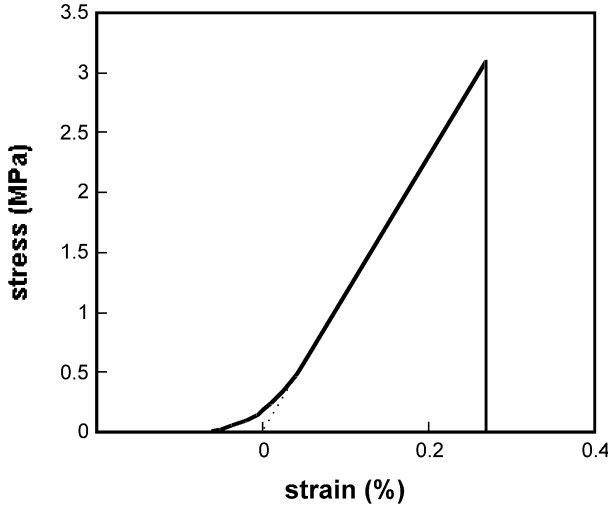

Fig. 2. Typical stress-strain curve of the set plaster obtained from a three point bending loading curve.

MPa). The main mechanical parameters evaluated for the neat plaster are a Young's modulus $E = 2.9$ GPa, a compression strength $\sigma_c = 12.8$ MPa and a toughness of 0.14 MPa$\sqrt{m}$.

4.2. Characterisation of the PA fibre-reinforced plaster

4.2.1. Setting of the materials

When plaster is mixed with water, the ensuing hydration reaction is exothermic. The progress of the reaction has therefore been followed using calorimetric measurements. The temperature rise ΔT during the plaster setting depends on the consistency and the concentration of calcium sulphate dihydrate formed. The temperature variations versus time during the plaster setting are plotted in Fig. 3 for the different composites under study. Three main features are noted:

(i) All the composite materials undergo an expansion during their setting, whereas the neat plaster was designed for a good dimensional stability. Therefore, the observed expansion of the composites is related to the fact that polyamide fibres are water-absorbent, so they may absorb water during the mixing sequence and the setting period, which results in the volume increase.

(ii) Association of fibres to the plaster extends the setting period and the increase of temperature is lower than for the neat plaster (Fig. 3a). Then we can notice that the rate of temperature increase and the plateau value are all the lower, and the setting period is all the longer, as the fibre concentration increases. These observations suggest that a total hydration of the plaster grains in the presence of polyamide fibres is not achieved at the end of the setting: the amount of water soaked up by the fibres is no more available for the plaster hydration

(iii) Fig. 3b shows that the plateau value of the temperature at the end of the setting period is correlated to the fibre length rather to its diameter.

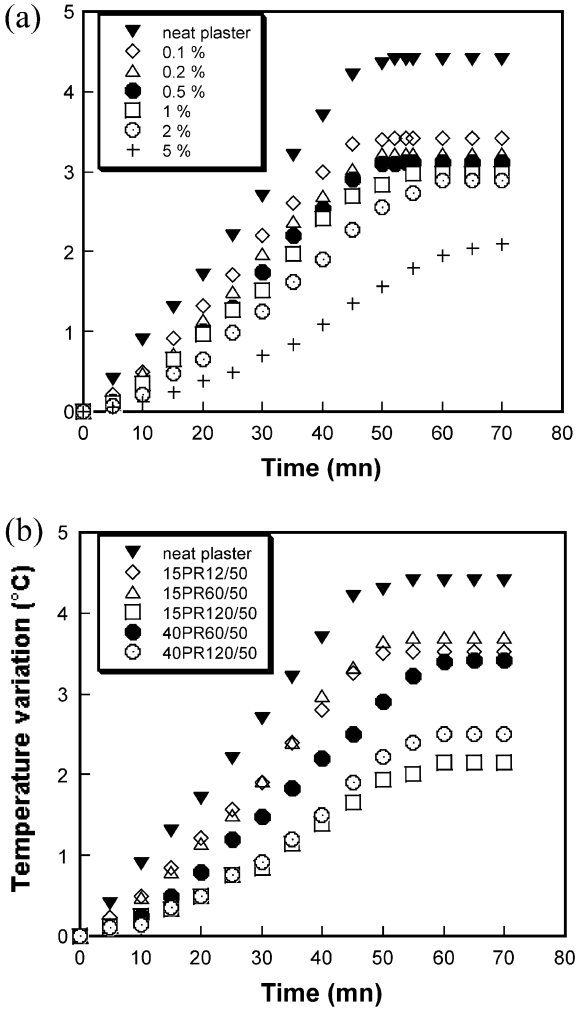

Fig. 3. Temperature variation with time during the setting of reinforced plaster: influence of the fibre concentration (a) and the fibre aspect ratio (b).

Furthermore, the absorbed water is partially released by the fibres as the specimens are dried in the oven at 40 °C. Thus a gap may appear between the fibres and the matrix (more likely a weak fibre-matrix bond), which will influence the load transfer onto the fibres.

4.2.2. Microstructural observations

Figs. 4 and 5 show examples of the fracture surfaces of the composites. The fibre-matrix interface appears very porous and consists of loosely bonded hydrated grains of plaster in contact with the fibres. The surfaces of the fibres totally pulled out of the matrix are smooth or show some debris of plaster but no obvious marks of adhesion. This loosely bonded fibre/matrix interface may be associated to the shrinkage of the polyamide fibres during the drying step.

Fig. 4. Evidence of a lack of total hydration of the gypsum grains (15PR60/1).

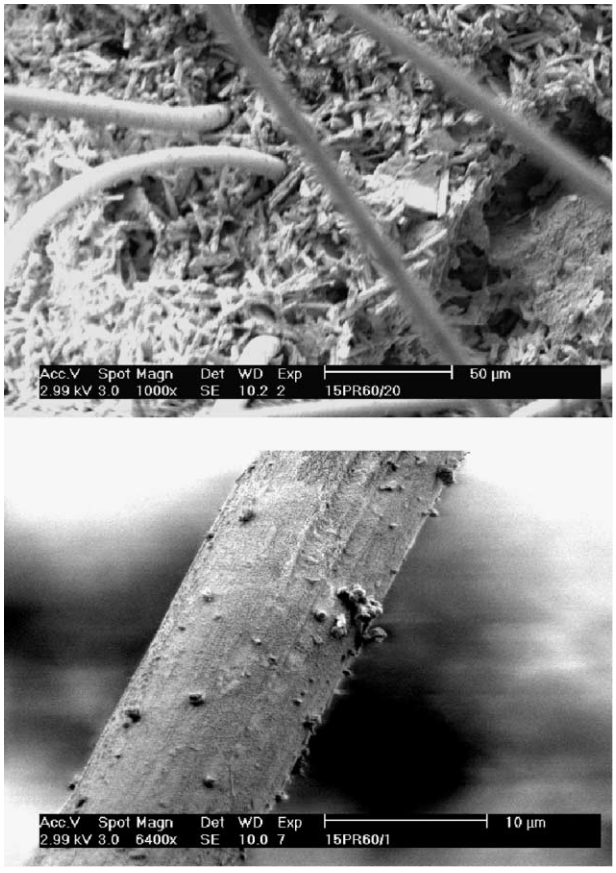

Fig. 5. Some aspects of the surfaces of the fibres pulled out of the plaster.

As a consequence of the rivalry for water between the plaster grains and the polyamide fibres, changes in the microstructure of the matrix around the fibres are noticed in comparison with the neat plaster: the density of needle-like crystallites is noticeably reduced. Moreover, as the concentration of fibres is increased, there is a propensity for the formation of paquets, with enclosed large pores and matrix-rich domains.

4.2.3. Monotonic loading curves of smooth specimens

For the same fibre length and a given concentration of reinforcement, we have noticed no difference between the loading curves of specimens made of fibres of diameter 15 or 40 μm. This is consistent with the analysis presented above about the influence of the fibre aspect ratio on the temperature variation during the setting. So the influence of the fibre aspect ratio reduces to the effect of the fibre length.

4.2.3.1. Damage growth. The stress–strain curves associated to the materials different by the concentration and the length of the fibres are depicted in Fig. 6. The composite with 0.1 wt.% of fibres behaves just like the neat plaster: the correlation of the loading curve with the acoustic emission signal in Fig. 7a reveals that no

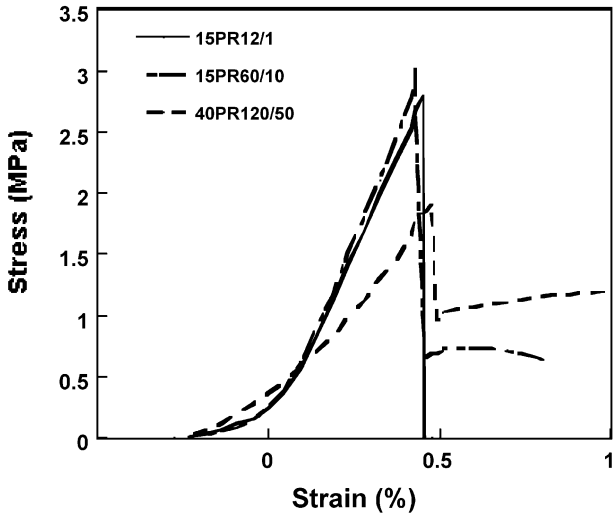

Fig. 6. Stress–strain curves associated to different composite materials: low concentration of short fibres 15PR12/1 (——), intermediate concentration of the middle length fibres 40PR60/10 (– - –) and higher concentration of the longest fibres 40PR120/50 (– • –).

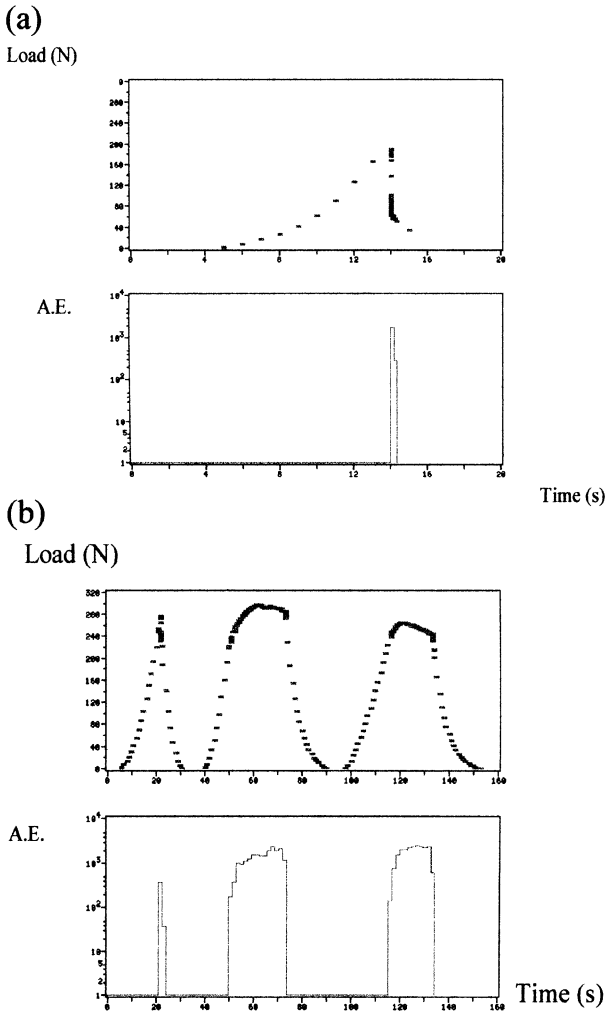

Fig. 7. Correlation of the total number of acoustic emission counts with the load vs time diagram for the neat plaster (a) and a composite material (b).

subcritical crack growth occurred prior to the maximum load point (ε_R, σ_R). At the opposite, with higher concentrations of fibres, upon loading a sudden crack propagation occurs as the critical point is reached (ε_R, σ_R), but the crack stabilises at a point (ε_R, σ_S); and the load still rises as the load point displacement is increased. At the onset of the first damage within the composites (matrix cracking), the load is transferred onto the fibres in the plane of the crack, which will be elastically stretched and progressively pulled out of the matrix.

Matrix multicracking is not observed as the fibres are randomly dispersed and are not strongly bonded to the plaster. Upon reloading the cracked specimen, acoustic emission starts again only when the applied stress reaches a critical value for matrix cracking in the remaining ligament (Fig. 7b). No acoustic emission is recorded upon unloading.

4.2.3.2. Mechanical parameters for smooth specimens. The matrix cracking strains measured on the different types of composites (Fig. 8a) fluctuate within the strain range associated to the neat plaster (0.35–0.51%). On the other hand, for all these materials, the evolution of the Young's modulus (Fig. 8b) shows a downward trend much more pronounced than the theoretical evolution derived from the application of the law of mixture (continuous line in Fig. 8b). The variations of the flexural and compression strengths (Fig. 8c and d) also show a downward trend whatever the aspect ratio of the reinforcement. These observations may be explained by the presence of a weak fibre-matrix interface; roughly, the location of the fibres can be regarded as pores within the plaster matrix).

4.2.3.3. Fibre efficiency factor (FEF). The major benefit of the presence of the fibres is to avoid a catastrophic failure of the material in two distinct pieces. Herein, the monotonic loading curves of the composites are analysed with a view to appraise the role of the fibres (Fig. 9a). The fibre efficiency factor is evaluated by the ability of the composite to overcome (stabilize) the first damage which occurs at (ε_R, σ_R). Once the composite is loaded up to this critical point (ε_R, σ_R), the strain energy W_S is available for the (i) initiation of a matrix crack which will propagate, while the bridging fibres rub against the matrix in the wake of the crack (ii), as they

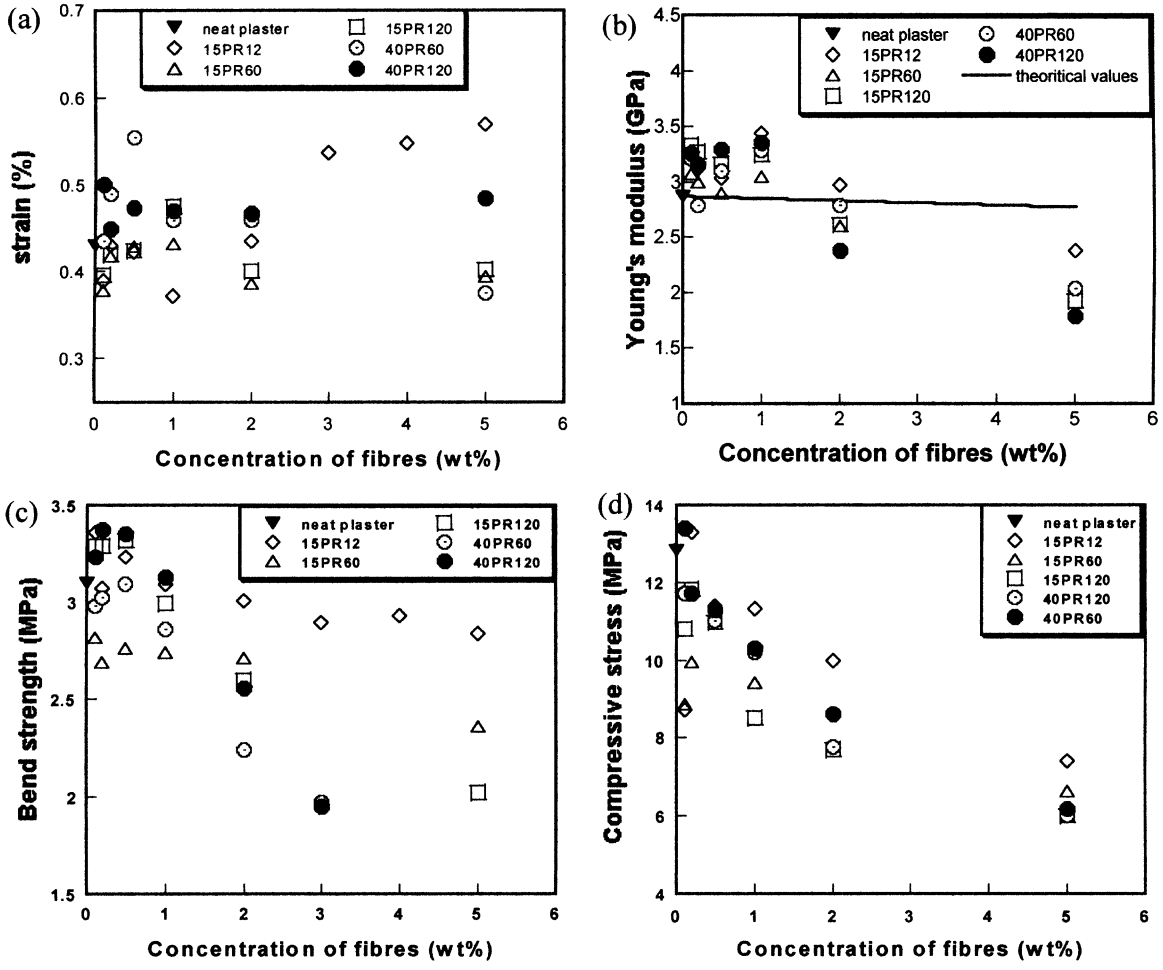

Fig. 8. Matrix cracking strain (a), Young's modulus (b), bend (c) and compression (d) strengths as a function of the fibre concentration and aspect ratio.

are stretched (iii). The efficiency of the dissipation mechanisms (ii) and (iii) depends on a few conditions : the relative values of the ultimate strains of the fibre and the matrix; the concentration of fibres must be higher than a critical value as they have to carry the excess load at the onset of matrix failure; the fibre/matrix interfacial shear stress must allow a good stress transfer onto the fibres, this requirement is related to the fibre aspect ratio.

So the crack stabilisation stress is likely a function of the micromechanical properties of the fibre-matrix interface, the concentration and the physical characteristics of the reinforcement.

We define the fibre efficiency factor FEF, by the ratio of the crack stabilisation stress (σ_S) to the material's strength σ_R (matrix cracking stress within the composite):

$$\mathrm{FEF} = \frac{\sigma_S}{\sigma_R} \tag{5}$$

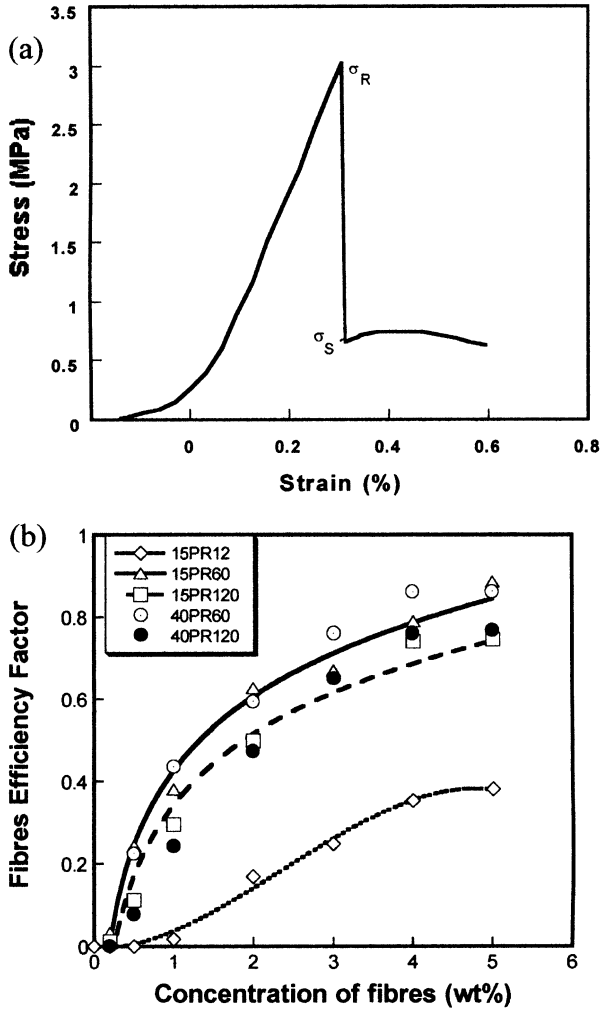

Fig. 9. (a) Typical stress–strain curve of a PA fibres reinforced plaster material (15PR60/10), (b) variation of the fibre efficiency factor with the fibre concentration and the aspect ratio.

The FEF of the different materials are plotted in Fig. 9b against the concentration of fibres. For one, the efficiency to overcome the first matrix cracking is the worst for the materials with the shortest fibres (15PR12) as these fibres hardly can bridge the matrix crack. Afterwards, the influence of the fibre length is much more noticeable than the diameter is, as it was mentioned about the variation of the flexural strength. For another, 6 mm long fibres are more efficient than 12 mm long fibres; this relates to the possible folding of the long fibres due to the elaboration method.

4.2.4. Fracture toughness

The variation of the fracture toughness of the different materials with the concentration of fibres up to 6 wt.%, is shown in Fig. 10. First, two types of behaviour are noted which highlight the influences of both the length and the concentration of the reinforcement. The materials with 6 mm long fibres exhibit a continuous upward trend in the range of fibre concentrations investigated. The curves associated to the composites with the shortest (1.2 mm) or the longest (12 mm) fibres rise for fibre concentrations below 2 wt.% and then decrease towards the toughness of the neat plaster as a consequence of the formation of zones of entanglement of the fibres. In both cases toughening occurs by two main mechanisms: matrix fracture and fibre sliding and pullout. The contribution of the latter mechanism depends directly on the total fibre length rubbing against the matrix, so the 1.2 mm long fibres contribute little to the dissipation of the elastic energy stored in the specimen. On the other hand, as the contribution of the 12 mm long fibres is weaker than the one of the 6 mm long fibres, we conclude that these fibres are probably folded.

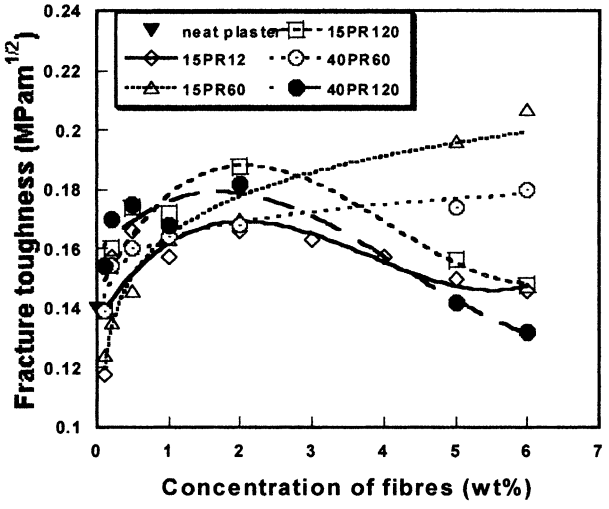

Fig. 10. Variation of the fracture toughness with the fibre concentration and aspect ratio.

5. Conclusions

This study was intended to check the availability of polyamide fibres as reinforcement of a commercial plaster. The presence of these water-absorbent fibres preclude the hydration of the gypsum grains located close to the fibres, perturbs the arrangement of the dihydrates and results in a weak fibre/matrix interface. This results in a reduction of Young's modulus and the flexural and compression strengths as the concentration of fibre increases. However, the first damage in the composite consists in matrix cracking, as testified by the critical strain value. We have defined a fibre efficiency factor which accounts for the ability of the composites to overcome the first matrix cracking. Analysis of the evolutions of this efficiency factor and the fracture toughness point out a very limited influence of the fibre diameter and an optimum fibre length.

Acknowledgements

The authors are indebted to BPB Placo, Center of Vaujours (France), for supplying of the gypsum. They gratefully thank Mrs Sylvie Perez, the Central Laboratory manager, for her suggestions and advice.

References

[1]. Gmouh, A., Samdi, A., Moussa, R. and Gomina, M., Lightened plaster-based composite materials: elaboration and mechanical properties. *Silicates Industriels Ceramic Science and Technology*. *66*, 61–66.

[2]. Gautherin C. and Morel C. *Mechanical Characterization of Plasters, Third Year Probation Report at the Engineering School E.N.S.I – Caen*. ISMRA (France)

[3]. Hernández-Olivares, F., Oteiza, I. and de Villanueva, L., Experimental analysis of toughness and modulus of rupture increase of sisal short fibres reinforced hemihydrated gypsum. *Composite Structures*, 1992, **22**, 123–137.

[4]. Coutts, R. S. P., Wastepaper fibres in plaster products. *J. Mater. Sci. Lett*, 1990, **10**, 77–78.

[5]. Singh, M. and Garg, M., Microstructure of Glass Fibre Reinforced Water Resistant Gypsum Binder Composites. *Cement and Concrete Research*, 1993, **23**, 213–219.

[6]. Wertz, S., Innovative Use of Glass Reinforced Gypsum. *The Construction Specifier*, 1990, **43**, 76.

[7]. Ali, M. A. and Grimer, F. J., Mechanical properties of glass fibre-reinforced gypsum. *J Mater Sci*., 1969, **4**, 389–395.